Two-Dimensional Communication of Networked Devices Through a Single Conductive Surface

Josep Rius

Abstract—**This paper shows the possibility of two-dimensional communication between electronic devices by using only one conductive surface. An analysis of the expected magnitude of the signal at the reception point as a function of distance and electrical parameters of the conductive surface is presented. Measurements on surfaces from 0.4 to 2.56 m^2 and with sheet resistances from 77 to 1462 ohm/square prove the correctness of this analysis. In addition, practical rules to locate and orient the transceivers are given. Prototype transceivers connected to a plane with one conductive surface able to communicate at 100Kbit/s at a distance of 2m are described.**

Index Terms— **computer networks, conducting films, data communication, distributed parameter circuits.**

I. Introduction

Most data communication applications are generally carried out by one-dimensional (wiring cables, interconnects, or fibers) or three-dimensional (wireless transmission through free space, gases or liquids) media, whereas communication by two-dimensional media is less considered. Surfaces, however, are ubiquitous in everyday life. Walls, tables, garments and floors are a few examples of the pervasive presence of surfaces. This ubiquity offers unique opportunities for electronic communication in applications where ordinary wire or wireless technologies may appear less attractive.

Communication through conductive surfaces has some of the benefits of wire and wireless technologies like easy networking, two-dimensional mobility of transceivers, power and signal paths and it is potentially not electrically disturbing. Moreover, this type of communication provides a robust connection between devices because there are multiple signal paths.

In the early years of this decade, several papers presented the concept of data transmission through two-dimensional media [1][2][4][6] and in the following years applications of this concept were published in the field of networked sensors [3-5], [7-9] and other fields such as clothing [10-12] and medicine [13, 14].

These proposals have in common that data transmission is always performed through *a pair* of conductive surfaces. Data propagate as an electromagnetic wave in the dielectric layer insulating the two conductive layers (or as a diffusive perturbation [6]) and are finally detected at the receiver point. Two conductive planes must be available, implying that: (a) a relatively complex and expensive fabrication process to generate and join the conductive layers at both sides of the insulation is involved (b) careful control during fabrication is required to avoid short-circuits between the conductive layers, (c) an unintentional short-circuit between the two conductive layers during operation may degrade or interrupt the communication, and (d) the interface between the electronic devices and both surfaces is relatively complex.

In contrast, data communication by a single conductive surface has the following benefits: (a) simpler and less expensive fabrication process because only one conductive layer is needed, (b) short-circuits are not an issue, and (c) the interface between the electronic devices and a single conductive layer is much less complex.

This approach (which, as far as the author knows, has not been previously proposed) is sketched in Figure 1. The signal from the transmitter **T** (we call it *transmitter dipole*) is a time-varying potential difference between two points of the single conductive sheet, namely x_{T1},y_{T1} and x_{T2},y_{T2}., which generates a time-varying, two-dimensional potential field on the conductive sheet that propagates to the receiver **R** (we call it *receiver dipole*), which is connected to the conductive sheet at points x_{R1},y_{R1} and x_{R2},y_{R2}. The potential difference between these two points, V_R, is the received signal.

The parameters of interest are the sheet resistance R_S and the parasitic capacitances (not shown in the Figure) between the conductive sheet and the surrounding bodies (Earth, metallic bodies, etc).

The goal of this paper is to show the feasibility of data transmission between networked devices using only one conductive surface as the transmission medium. Furthermore, the expected amplitude of the received signal as a function of plane dimensions, electrical parameters and transmitter and receiver sizes and distances, as well as the implications of this approach for data transmission in terms of speed and power consumption of the connected devices are analyzed.

This work was supported in part by the Comisión Interministerial para la Ciencia y la Tecnología under Project TEC2007-66672, and the Spanish Secretaría de Estado de Educación, Universidades y Desarrollo.

J. Rius is with the Dept. d'Enginyeria Electrònica of Universitat Politècnica de Catalunya, 08028 Barcelona, Spain, (phone: 34 934016650, fax: 34 934017785; email: rius@eel.upc.edu).

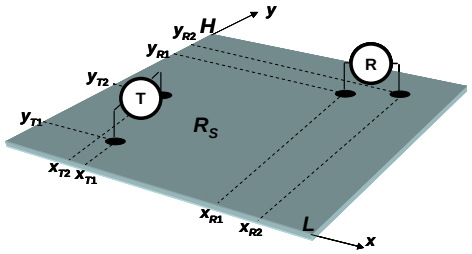

Fig. 1. Plane with only one conductive surface.

The paper is organized as follows: Section 2 derives formulas to calculate the voltage at the receiver dipole when the transmitter dipole injects/withdraws a constant current elsewhere. Section 3 analyzes the same problem when the excitation is a time-varying current. In this case, the analysis is extended to planes with one and two conductive surfaces. Section 4 provides experimental results obtained from several samples of planes with one and two conductive surfaces and compares them with the analytical results of Sections 2 and 3. It also presents a prototype implementation of a communication system built on one of the samples. In Section 5, the main relationships between sheet resistance, power consumption, speed and dimensions of the communication system are investigated. Finally, Section 6 summarizes the work and draws conclusions.

II. Static Analysis

In static conditions, the potential difference V_R at the receiver electrodes is independent of time. This potential difference as a function of the surface size and shape and the physical parameters can often be calculated by numerical methods only. However, for simple geometries, like rectangular ones, it is possible to derive closed form expressions for V_R. This is the goal of this Section.

The problem can be divided into three parts, namely obtaining the potential at any single point on the surface of an infinite isolated conductive strip caused by two filament lines which inject and withdraw a constant current into and from the strip at two given points; generalizing this result to a rectangular surface, and finally deriving a closed form expression for the potential difference (voltage) between two arbitrary points on the rectangular surface.

A. *Potential at any point on an infinite isolated strip caused by the injection/withdrawal of current at two arbitrary points*

Figure 2 sketches the geometry of the problem. We first derive a formula for the potential at a point P produced by two current filaments of infinite length and constant magnitude I and $-I$ at points $(a,0)$ and $(b,0)$ in a conductive medium limited by two surfaces A and B of infinite extent in y and z directions. With these conditions, the problem becomes two-dimensional and the region of interest is the strip of width L and infinite length limited by lines A and B. The current enters the strip at point $(a,0)$ and leaves it at point $(b,0)$. No current crosses A and B. The electrical parameter defining the conductive medium in the strip is its sheet resistance R_S.

Let the origin of the complex plane be 0, and P the point $z = x + jy$. The images of the current lines are shown at points z_{1+}, z_{-1+}, z_{2+}, z_{-2+}, … and z_{1-}, z_{-1-}, z_{2-}, z_{-2-}, etc. whose distances from P are r_{1+}, r_{-1+}, r_{2+}, r_{-2+}, … and r_{1-}, r_{-1-}, r_{2-}, r_{-2-}, etc. The potential at P caused by the currents at a and b and the induced images will be calculated from the current itself and its infinite set of images. The total potential at P is a sum of expressions, one for each current, as shown by equation (1):

$$V_P = -\frac{IR_S}{2\pi} \ln \prod_{n=-\infty}^{\infty} \frac{r_{n+}}{r_{n-}} \tag{1}$$

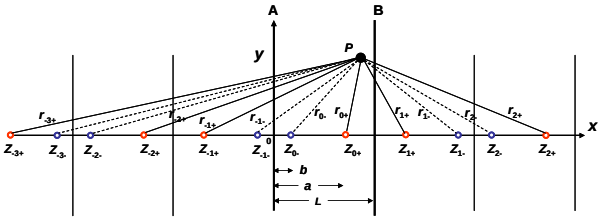

Fig. 2

According to [15] and [16], we can develop the infinite product of (1) to obtain the following closed form expression:

$$V_P = \frac{-IR_S}{2\pi} \mathrm{Re}\left\{ \ln \frac{\sin\left(\pi \frac{z+a}{2L}\right) \sin\left(\pi \frac{z-a}{2L}\right)}{\sin\left(\pi \frac{z+b}{2L}\right) \sin\left(\pi \frac{z-b}{2L}\right)} \right\} \tag{2}$$

where $\mathrm{Re}\{\cdot\}$ denotes the real part. Now, in order to find the potential in a rectangular plane, we need to generalize this result.

B. *Potential in a rectangular plane*

Imagine a pair of filament wires of infinite length intersecting a perpendicular rectangular plane of dimensions L, H at points $z_+ = x_+ + jy_+$ and $z_- = x_- + jy_-$. The wires inject and withdraw a constant current I and $-I$ into and from the plane, respectively. Let the origin of the complex plane be identified as 0, P the point $z = x + jy$ and the four sides of the plane be isolated. For the case of the rectangular plane the potential at P can be obtained by generalizing formula (2) in the previous sub-section.

In this case there is an infinite number of horizontal rows of images for each current which must be considered to obtain the desired boundary conditions of zero current at the sides of the rectangle of vertices (0,0), (L,0), (L,H) and (0,H).

Therefore, the total potential at point P results from the addition of eight contributions: four due to an infinite number of horizontal rows of images of the positive current, and four due to an infinite number of horizontal rows of images of the negative current. The double periodicity of the images suggests the use of elliptic functions [16] to obtain V_P. The result is the following closed form equation (3):

$$V_P(z) = \frac{-IR_S}{2\pi} \mathrm{Re}\left\{ \ln \frac{\vartheta_1\left(\pi \frac{z-z_+}{2L}\right) \cdot \vartheta_1\left(\pi \frac{z+z_+}{2L}\right) \cdot \vartheta_1\left(\pi \frac{z-\bar{z}_+}{2L}\right) \cdot \vartheta_1\left(\pi \frac{z+\bar{z}_+}{2L}\right)}{\vartheta_1\left(\pi \frac{z-z_-}{2L}\right) \cdot \vartheta_1\left(\pi \frac{z+z_-}{2L}\right) \cdot \vartheta_1\left(\pi \frac{z-\bar{z}_-}{2L}\right) \cdot \vartheta_1\left(\pi \frac{z+\bar{z}_-}{2L}\right)} \right\} \tag{3}$$

where the hat above z_+ and z_- denotes the complex conjugate and the elliptic theta function $\vartheta_1(\cdot)$ with parameter $q = \exp(-$

$\pi H/L$) is a standard built-in function (like trigonometric ones) in any computer algebra system.

C. Potential difference at the receiver dipole

Now the potential difference V_R between points R1 and R2 of Figure 1 can be calculated as the real part of the difference between two logarithms. That is,

$$V_R(z)=\frac{-IR_S}{2\pi}\mathrm{Re}\left\{\left.\ln\frac{\vartheta_1\left(\frac{\pi}{2L}(z-z_+)\right)\cdot\vartheta_1\left(\frac{\pi}{2L}(z+z_+)\right)\cdot\vartheta_1\left(\frac{\pi}{2L}(z-\bar{z}_+)\right)\cdot\vartheta_1\left(\frac{\pi}{2L}(z+\bar{z}_+)\right)}{\vartheta_1\left(\frac{\pi}{2L}(z-z_-)\right)\cdot\vartheta_1\left(\frac{\pi}{2L}(z+z_-)\right)\cdot\vartheta_1\left(\frac{\pi}{2L}(z-\bar{z}_-)\right)\cdot\vartheta_1\left(\frac{\pi}{2L}(z+\bar{z}_-)\right)}\right|_{z=z_{R1}}\right.$$
$$\left.-\left.\ln\frac{\vartheta_1\left(\frac{\pi}{2L}(z-z_+)\right)\cdot\vartheta_1\left(\frac{\pi}{2L}(z+z_+)\right)\cdot\vartheta_1\left(\frac{\pi}{2L}(z-\bar{z}_+)\right)\cdot\vartheta_1\left(\frac{\pi}{2L}(z+\bar{z}_+)\right)}{\vartheta_1\left(\frac{\pi}{2L}(z-z_-)\right)\cdot\vartheta_1\left(\frac{\pi}{2L}(z+z_-)\right)\cdot\vartheta_1\left(\frac{\pi}{2L}(z-\bar{z}_-)\right)\cdot\vartheta_1\left(\frac{\pi}{2L}(z+\bar{z}_-)\right)}\right|_{z=z_{R2}}\right\} \quad (4)$$

Expression (4) is the final closed form solution of the potential difference at the receiver electrodes when the transmitter dipole injects/withdraws a constant current.

III. Dynamic analysis

When a time-varying current is applied at the transmitter electrodes, the signal captured by the receiver has a smaller amplitude than in the static case. The purpose of this section is to obtain expressions for this amplitude as a function of the electrical parameters and dimensions of the rectangle, and as a function of the signal frequency.

A. Solution for an infinite plane

Let us first find the potential at a point P placed at distance r from the origin of an infinite plane when a steady-state sinusoidal current $I_0\exp(j\omega t)$ is injected at the origin. The plane has the following parameters: sheet resistance, R_S [Ω/square], and capacitance per unit area, C_a [F/cm^2]. Equation (5) [17] shows the final result:

$$V_P=\frac{I_0R_S}{2\pi}e^{j\omega t}K_0\left((1+j)\frac{r}{\delta}\right),\qquad \delta=\sqrt{\frac{2}{\omega R_S C_a}} \quad (5)$$

where $K_0(z)$ is the modified Bessel function of second kind and argument z [18], and the characteristic length δ is identified as the diffusion length of the signal in the plane. Expression (5) gives the potential at P as a time harmonic function whose attenuation with distance depends on the fraction r/δ. This equation can be simplified in the following two limiting cases.

The first is when $r/\delta\to 0$, that is, we consider only distances r from the origin much smaller than the diffusion length δ. In this case, the following asymptotic expression for $K_0(z)$ holds [18]:

$$K_0\left((1+j)\frac{r}{\delta}\right)\to\ln\frac{\delta\sqrt{2}}{r}-j\frac{\pi}{4} \quad (6)$$

The second limiting case is the opposite. If $r/\delta\to\infty$, that is, the distance from the origin is large compared with δ, or, for a given distance, the signal frequency is very high, then the following asymptotic expression holds [18]:

$$K_0\left((1+j)\frac{r}{\delta}\right)\to\sqrt{\frac{\pi}{4}\frac{\delta}{r}}e^{-\frac{r}{\delta}}e^{-j\left(\frac{r}{\delta}+\frac{\pi}{4}\right)} \quad (7)$$

Both cases are significant for the purpose of this paper. For instance, if the plane dimensions are much smaller than the diffusion length, the static analysis of Section 2 holds. A steady-state sinusoidal signal injected at a point reaches a receiver placed at any other point in the finite plane substantially with the same amplitude as when it is transmitted. On the contrary, if the dimensions of the finite plane are large compared with δ, the transmitted signal damps exponentially with distance and is received only at a small neighborhood of the transmitter. Remember that δ depends on the frequency. Thus, given the plane dimensions, this parameter determines the maximum frequency of the signal that can be transmitted through the whole plane with low attenuation.

B. Solution for a rectangle

From expression (5) and by using the method of images it is possible to obtain a general expression for the potential measured at any point in a finite plane of dimensions $L\times H$. This potential can be calculated by adding the contribution of the currents at the image points of an infinite set of adjacent planes, all of dimensions $L\times H$.

According to (5), it is clear that the potential at P is the sum of the current contribution and of all its images, as expression (8) shows:

$$V_P=\frac{I_0R_S}{2\pi}e^{j\omega t}\sum_{n,m=-\infty}^{+\infty}K_0\left(\frac{r_{nm}}{\delta'}\right),\qquad \delta'=\frac{\delta}{1+j} \quad (8)$$

where r_{nm} is the distance between P and image nm.

The previous analysis solves the problem for the case of a transmitter connected at one point in a plane with one or two conductive surfaces. The analysis is now extended to the case of a transmitter connected at two points in a plane with only one conductive surface (Figure 1).

We start with expression (8), which shows the potential at a point P in a finite plane caused by a current source I_0 injected at a given point, for example T1. By superposition, we obtain the potential at P when there is a current sink of value $-I_0$ at another point, for example T2. Using the same technique, we obtain the potential at a point N produced by the same current source and sink. The points of application of the current source/sink are the locations of the transmitter dipole contacts, T1 and T2, and points P and N are the locations of the receiver dipole contacts, R1 and R2. Following this process, for the voltage at the receiver dipole $V_R = V_P - V_N = V_{R1} - V_{R2}$ we have

$$V_R=\frac{I_0R_S}{2\pi}e^{j\omega t}\left\{\sum_{n,m=-\infty}^{+\infty}\left[\left(K_0\left(\frac{r_{nm,pp}}{\delta'}\right)+K_0\left(\frac{r_{nm,nn}}{\delta'}\right)\right)-\left(K_0\left(\frac{r_{nm,np}}{\delta'}\right)+K_0\left(\frac{r_{nm,pn}}{\delta'}\right)\right)\right]\right\} \quad (9)$$

where $r_{nm,ij}$ denotes the distance between the point i of the image current nm and the contact j of the receiver dipole,

being $i \in \{p \equiv T1, n \equiv T2\}$ and $j \in \{p \equiv R1, n \equiv R2\}$.

IV. Experimental Results

This Section presents several experiments with planes of different sizes and electrical parameters to check the theory in Sections II and III. Table I summarizes the dimensions and parameters of three of these planes.

TABLE I.

Plane #	L [cm]	W [cm]	R_s [Ω/□]	C_a [F/cm^2]	# of cond. surf.	Case
1	140	73.6	1462	163×10^{-15}	2	Dynamic
2	73.6	54.4	1462	14×10^{-15}	1	Static/Dynamic
3	210	122	528	9.3×10^{-15}	1	Static/Dynamic

A. Results for plane #1

This plane consists of a pair of sheets of conductive paper adhered to both sides of a 0.5cm thick, 140cm long, 73.6cm wide foam plate. That is, this plane has two conductive surfaces. A pair of contacts (one at each side) in the center of each sheet connects the transmitter. The measurement points (receiver contacts) are at fifteen places distributed in the following way: seven points separated by 10cm and placed between the center and the short side of the rectangle (*horizontal* points); five contacts separated by 10cm and placed in diagonal (*diagonal* points); and three contacts separated by 10cm and placed between the center and the long side of the rectangle (*vertical* points). All contacts are connected to both sides of the plane by circular copper discs with a radius of 1.3cm.

An Agilent 33120A Function Generator provides the transmitter contacts with a sinusoidal voltage with a constant amplitude of 1Vpp at the following twelve frequencies: 1KHz, 10KHz, 20KHz, 50KHz, 100KHz, 200KHz, 500KHz, 1MHz, 2MHz, 5MHz, 10MHz and 15MHz. Two differential probes Tektronix P6247 connected to a TEKTRONIX TDS7000 Digitizing Oscilloscope measure both the signal amplitude at the centered contacts and the amplitude at the other receiver contacts.

The solid lines in Figure 3 represent the amplitudes at the *horizontal* points calculated with expression (8), and the circles represent the measured amplitudes. The upper and decay lines correspond to the lower and higher frequencies, respectively. Results for the *diagonal* and *vertical* points are similar. As can be seen, the agreement is very good for the lower and higher frequencies and less good but still remarkable for the 50KHz, 100KHz and 200KHz frequencies.

It is interesting to observe how the voltage at the transmitter contacts (circles in the top left corner of Figure 3, is not constant but depends on the frequency. This phenomenon is explained by considering the two conductive surfaces as the plates of a capacitor. The signal from the Function Generator is applied to a capacitive load, so its internal output impedance (50Ω) and the capacitor form a frequency-dependent voltage divider that attenuates the effective signal amplitude at the transmitter contacts.

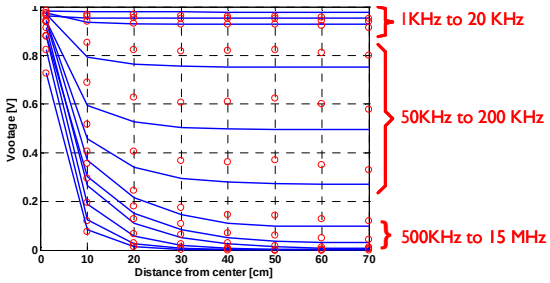

Fig. 3. Voltage amplitudes at the seven *horizontal* points of plane #1. Solid lines: calculated voltage at each point, circles: measured.

Also note the correctness of the analysis in the previous section. At high frequency (small diffusion length δ) the signal is strongly attenuated with distance whereas at low frequency (large diffusion length) the attenuation is small and the signal received at any place has practically the same amplitude as the transmitted signal.

B. Results for plane #2

This plane consists of a 73.6cm long, 54.4cm wide single sheet of conductive paper lying on top of a wooden platform. The contacts of the transmitter dipole are copper discs with a radius of 1.3cm placed near the corners of one of the short sides of the plane and separated by 40.8 cm. The contacts of the receiver dipole are made up of a pair of copper discs with a radius of 0.3cm separated by 1.8cm. The signal received by the dipole is measured at 49 places equally distributed over the plane.

For the static measurements, a constant voltage source is connected to the transmitter dipole contacts and a voltmeter measures the voltage at the receiver dipole. For the dynamic measurements, as in plane #1, the sinusoidal input signal is generated by the Function Generator with a constant amplitude of 1.8Vpp at the following frequencies: 1 KHz, 10 KHz, 20 KHz, 50 KHz, 100 KHz, 200 KHz, 500 KHz, 1 MHz, 2 MHz, 5 MHz, 10 MHz and 15 MHz. The differential probes simultaneously measure the voltage amplitude at the transmitter dipole and at the receiver dipole.

1) Static measurements

In the static measurements, the transmitter dipole is connected to a constant voltage source of 10V injecting a constant current of 3.03mA. A voltmeter measures the potential difference between the pair of contacts of the receiver dipole. Two series of measurements reveal the influence of the orientation of the axis of the receiver dipole with respect to the axis of the transmitter dipole. The first series shows the voltage at the receiver dipole when it is oriented in the same direction as the transmitter dipole, that is, they are parallel. The second series shows the voltage at the receiver dipole when it is perpendicular to the transmitter

dipole. We call the first orientation *parallel* and the second *perpendicular*. Figures 4 and 5 summarize the results of both series.

Figure 4 is a logarithmic plot of the voltage at the receiver dipole for the 7x7=49 points on the surface for *parallel* orientation. In this case, the voltage is always positive. The filled surface is the value calculated from formula (4) and the dots represent the measured values. Notice that the agreement is very good.

Figure 5 provides the same results for *perpendicular* orientation. Now the voltage is positive or negative depending on the measurement point. The filled surface shows the calculated values and the dots the measured ones. Again, the agreement is excellent. This illustrates the importance of the relative orientation of transmitter and receiver dipoles. In these Figures the X and Y axis are the indices of the 7x7 places of the measuring points.

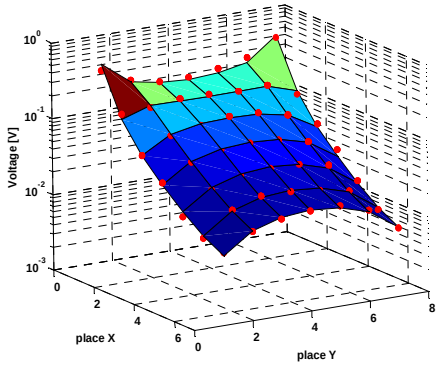

Fig. 4. Voltage at the receiver for static measurements on plane #2. *Parallel* orientation. Filled surface: calculated from (4), dots: measured.

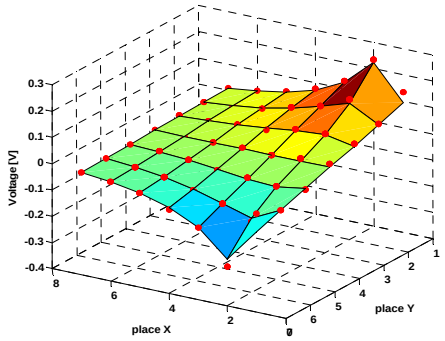

Fig. 5. Voltage at the receiver for static measurements on plane #2. *Perpendicular* orientation. Filled surface: calculated from (4), dots: measured.

2) Dynamic measurements

In the dynamic measurements, the Function Generator is connected at the same place as the voltage source in the static measurements. The amplitude of the generated voltage is 1.8Vpp. A differential probe connected to the oscilloscope measures the signal amplitude at the receiver dipole. Both dipoles have *parallel* orientation.

Figure 6 compares measured and calculated values at each of the 49 measurement points at 5MHz. The squares and the circles represent the values calculated by expression (9) and the measured values, respectively. The response at other frequencies is similar to that shown in this Figure. Again, X and Y-axis are the indices of the 7x7 measuring points.

As can be seen, the agreement is very good for most points. The differences between calculations and measurements can be explained by the non-uniformities of the electrical parameters and unavoidable uncertainties in the measurement of low-level signals. The relatively large deviation at the farthest points observed in Figure 6 is due to the small amplitude of the receiver signal (less than 1mV), which is lower than the electrical noise captured by the oscilloscope, whose averaging and synchronizing capabilities were stretched to the limit.

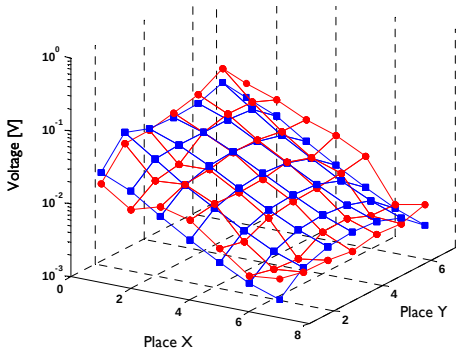

Fig. 6. Voltage amplitudes calculated (squares) and measured (circles) on plane #2 at 5MHz.

C. Results for plane #3

Plane #3 consists of a 2cm thick, 210cm long, 122cm wide wooden platform covered with a layer of conductive paint. The transmitter dipole is close to the two corners of one of the short sides of the plane. As in planes #1 and #2, the transmitter contacts are circular copper discs with a radius of 1.3cm. For plane #3 only dynamic measurements are shown.

In this case, the waveform supplied by the Function Generator is a rectangular signal of frequency 100 KHz and 5Vpp amplitude. A differential probe connected to the oscilloscope measures the signal amplitude at the receiver dipole.

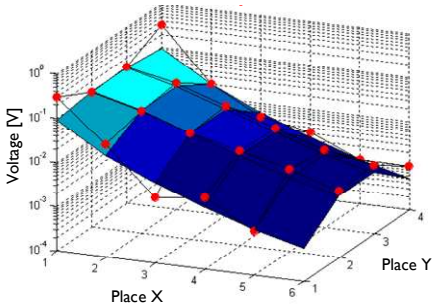

Fig. 7. Voltages measured and calculated on plane #3 with *parallel* orientation of dipoles.

Figures 7 and 8 compare values measured and calculated at each of the 6x4=24 measurement points for *parallel* and *perpendicular* orientation of dipoles, respectively. As far as perpendicular orientation is concerned, Figure 8 shows the

absolute value of the voltage at the receiver dipole. The circles and the filled surfaces are measured values (in V) and values calculated by expression (9), respectively.

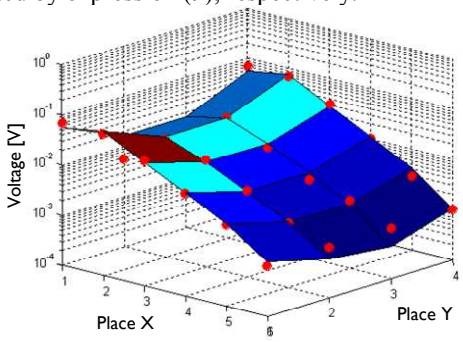

Fig. 8. Absolute value of voltage measured and calculated on plane #3 with *perpendicular* orientation of dipoles.

The agreement between measured and calculated values is very good, thus supporting the correctness of the analyses in Sections 2 and 3.

D. Prototype of communication network using only one conductive surface

We built a prototype of a communication system as an experimental platform to check the validity of our proposal. It is currently composed of transceivers connected to a PC and communicated through the conductive surface of plane #3 at 100Kbit/s. Standard protocols are used in a half duplex bidirectional communication. Figure 9 shows a photograph of the test bench.

Fig. 9. Test bench of a prototype of a communication system using a single conductive surface. Left: transmitter, right: receiver.

V. Maximum Frequency, Distance and Power Consumption

This Section analyzes the relationships between the size and material properties of planes with only one conductive surface, and important characteristics of any transmission system, such as maximum speed available, maximum distance between transmitters and receivers and power/energy consumption of devices. First, we examine the relationships between the current injected into the surface by the transmitter and its sheet resistance. Both magnitudes are related to power consumption. Next, we explore the relationships between the transmitter and the receiver dipole dimensions, distance between them and maximum speed available.

A. Current, sheet resistance and power consumption

It is clear that the resistivity of materials used to cover the transmission surface strongly influences the features of the transmission system. On the one hand, if the resistivity is very high (surfaces with very high sheet resistance), nothing can be transmitted because the current injected by the transmitter becomes zero. On the other hand, materials like metals with very low resistivity (surfaces with very low sheet resistance) are not particularly useful for transmission either, because they behave as short-circuits, thus overloading the transmitter circuits. However, using the proposed approach a range of values for surface sheet resistance becomes suitable for communication. This range is not analyzed in this paper. Instead, this sub-section presents some measured results obtained from surfaces with different sheet resistances.

Equations (4) and (9) show that the voltage at the receiver dipole is proportional to the product IR_S, where I is the current injected by the transmitter and R_S is the sheet resistance. In fact, the transmitter signal is usually injected into the conductive surface as a voltage V_0 applied to the transmitter connections. Thus, by Ohm's law current I is $I = V_0/R_T$, where R_T is the load resistance as seen from the transmitter contacts which in turn is proportional to R_S. Thus, if we measure R_T, expressions (4) and (9) can be written as a function of V_0 instead of I. Let us now look at some experimental relations between R_S, V_0 and power consumption, and at an estimation of the total energy consumed in the transmission.

Tables II and III summarize these results. The first and second columns identify the measured plane and its size. Planes #2 and #3 are the same as in Section IV. Plane #4 is of a similar size to that of plane #3, but the former is painted with a more conductive paint. The third column shows the sheet resistance of the conductive surface. The fourth column is the measured resistance between the transmitter contacts, R_T. The fifth column shows the voltage V_0 applied to the transmitter contacts in the static/dynamic measurements. The sixth column is the resulting current injected by the transmitter I_T, and the seventh contains the power supplied by the power supply, $P_T = V_0 \times I_T$. Tables II and III show the above data for the static and dynamic experiments respectively.

TABLE II.

Plane #	***L*×*W* [cm]**	***R*S [Ω/□]**	***R*T [Ω]**	***V*0 [V]**	***I*T [mA]**	***P*T [mW]**
2	73.6×54.4	1462	3300	10	3.03	30.3
3	210×122	528.7	255	5	19.6	98
4	244×122	77	43	2.2	50.4	109

TABLE III.

Plane #	***L*×*W* [cm]**	***R*S [Ω/□]**	***R*T [Ω]**	***V*0 [Vpp]**	***I*T [mA]**	***P*T [mW]**
2	73.6×54.4	1462	3300	1.8*	0.55	0.98**
3	210×122	528.7	255	5*	19.6	98
4	244×122	77	43	1.6*	37.2	59.5**

* in planes #2 and #4 the applied signal is sinusoidal, so we take the amplitude. In plane #3 the signal is rectangular.
** this number is the maximum instantaneous power; the average power value is lower.

B. Time and energy estimation

From the data of Table III and by assuming a given transmission speed, we can estimate the energy consumed per

transmitted bit as ET = PT×T, where ET is the energy in J and T is the time of one bit in seconds. Therefore, assuming, for instance, that a digital signal of 5V amplitude is transmitted at a speed of 100Kbit/s, we have the energy per bit, as shown in Table IV for the tested planes.

TABLE IV.

Plane #	P_T [mW]	Energy per bit [μJ]
2	7.6	0.076
3	98	0.98
4	581	5.81

The total energy spent in sending a message depends on the number of bits of the message. If the message length is, say, 100 bits, the energy consumption per message is between 7.6 and 581 μJ. In the worst case, by taking 1mJ as the limit of the energy spent per message by a transmitter connected to plane #4, about 10^6 messages can be sent before fully discharging an off-the-shelf AA battery for portable devices. This number may be acceptable for many applications. Of course, if planes #2 or #3 are used, the number of messages increases by orders of magnitude.

The transceiver has other sources of power consumption when it is operating or in standby, implying that low power digital design techniques must be used to reduce these contributions to a minimum. In addition, when no data are transmitted, specific circuits connected to the plane should restore the energy lost by the transmitters. Nevertheless, the purpose of this sub-section is only to show the feasibility of transmitting data with an acceptable low power consumption using a single conductive surface. For this reason, techniques for low power circuit design or for remote power transmission are not analyzed here.

C. Size, distance and orientation of transmitter/receiver

Equations (4) and (9) determine the relationships between the distance and size of the transmitter/receiver dipoles and the amplitude of the received signal. These relationships are contained in the arguments of the theta functions in (4) and the Bessel functions in (9), but these expressions are too complex to allow direct conclusions to be drawn. Instead, an approximate interpretation obtained from these equations and confirmed by the experiments on the tested planes is given next.

If the signal frequency is sufficiently low (which means $r<<\delta$, see Section III), the amplitude of the received signal V_R can be calculated from (4). The following rules hold for the amplitude of the received signal in these conditions:

(*i*) If the distance between the transmitter contacts D_T or the receiver contacts D_R is of the order of magnitude of the plane size, then V_R approximately decreases exponentially with the distance between the centers of the transmitter and receiver dipoles, d_{TR}. However, if the effect of the boundaries is neglected (the plane can be considered as infinite) and $D_T + D_R << d_{TR}$, then the decrease is only approximately quadratic with d_{TR}. (*ii*) V_R is approximately proportional to the product $D_T \times D_R$. That is, doubling the distance between the transmitter or receiver contacts, the amplitude of the received signal is roughly doubled. Consequently, in the tested planes the contacts of the transmitters are well separated and placed close to the corners of one side of the planes. (*iii*) V_R reaches its maximum value at a given point on the surface when the receiver dipole is oriented in the same direction as the maximum gradient of the potential field created by the transmitter at that point. (*iv*) The reciprocity theorem holds, and therefore it is possible a bidirectional communication between the networked devices.

Let us examine the results obtained from measurements on the tested planes. Table V identifies the planes and summarizes their electrical parameters in columns 1-3. Column 4 lists the distance between the transmitter contacts D_T and their radius r_T. Column 5 gives the above parameters for the receiver dipole, D_R and r_R. Column 6 contains the distance between the centers of the transmitter and receiver dipoles d_{TR}, and column 7 shows the amplitude of the voltage measured at the receiver dipole V_R. The dipole axes are oriented in *parallel* and the transmitter is connected at the same points as in the experiments of Section 4. The frequency is 100 KHz, which guarantees that all distances are well below δ. The amplitude of the transmitted signal to each plane, V_0, is the same as in Table III.

TABLE V.

Plane #	R_S [Ω/□]	C_a [fF/cm^2]	D_T,r_T [cm]	D_R,r_R [cm]	d_{TR} [cm]	V_R [mV]
2	1462	14	40.8, 1.3	1.8, 0.3	54	1.4
3	528.7	9.3	105, 1.3	3.6, 0.3	198	3.65
4	77	10.1	108, 1.3	1.8, 0.3	228	0.71

It can be observed that, for similar d_{TR} and D_T, the amount of received signal V_R is about five times larger in plane #3 than in plane #4. This is mainly due to the combination of greater V_0 and D_R in plane #3. Also, note that planes #2 and #4 have similar V_0 and the same D_R. They have different D_T and d_{TR} but, comparatively, the transmitter and the receiver are closer in plane #2 than in plane #4, so V_R is greater in plane #2.

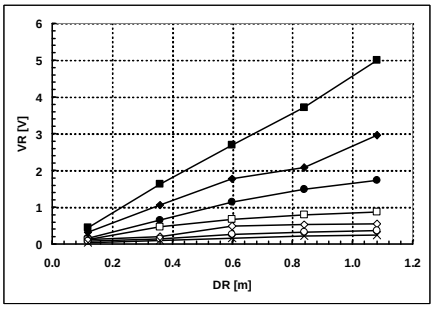

Fig. 10. V_R as a function of D_R taking d_{TR} as a parameter. Plane #3. Upper line: d_{TR} = 0m, lower line: d_{TR} = 1.44m.

Figures 10 and 11 show how received voltage obeys rules (*i*) and (*ii*). The V_R measured in plane #3 is shown as a function of D_R and d_{TR}. The transmitter is connected near the

corners of one short side of plane #4 and D_T = 105cm. The frequency is 100KHz and V_0 = 5Vpp. The dipole axes are oriented in *parallel*.

Figure 10 plots V_R as a function of D_R for seven equally spaced values of d_{TR} from 0 to 1.44m. As can be seen, there is a practically linear relation between V_R and D_R. Figure 11 illustrates the dependency of V_R on d_{TR} for five equally spaced distances D_R from 0.12m to 1.08m. Here, the exponential decrease of V_R is clearly observed.

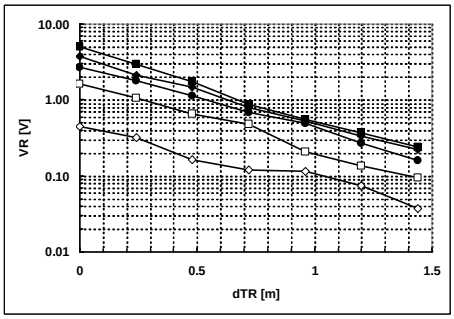

Fig. 11. V_R as a function of d_{TR} taking D_R as a parameter. Plane #3. Upper line: D_R = 1.08m, lower line: D_R = 0.12m.

VI. Conclusions

The purpose of this paper is to show how data transmission between networked devices is possible by using only a single conductive surface. The amplitude of the received signal and the transmission speed in rectangular planes with one or two conductive surfaces are analyzed as a function of electrical parameters and dimensions. Measurements on planes with a size between 73.6×54.4cm and 244×122cm and with sheet resistances from 77 to 1462 Ω/square corroborate the validity of the analysis. Practical rules to locate and orient the transceivers are given. Successful experiments demonstrate the feasibility of communications between networked devices using a single conductive surface with prototype transceivers, which can communicate at 100Kbit/s at a distance of 2m in a plane of 2.56 m^2. Issues as remote power transmission or contact less coupling of transceivers to the conductive surface are on going work not covered in this paper. Potential applications of this approach are in the fields of surface testing, home automation and wearable computing.

Acknowledgment

The author would like to thank students Vicenç Casadevall and Francesc Bonjoch for their help in making measurements on planes #2, #3 and #4.

References

[1] F. Scott, F. Hoffmann, M. Adledsee, G. Mapp, A. Hopper, "Networked Surfaces: a New Concept in Mobile Networking, *Proceedings of Third IEEE Workshop on Mobile Computing Systems and Applications,* IEEE, December 2000.

[2] K. Van Laerhoven, N. Villar, A. Schmidt and H.-W. Gellersen, "Pin@Play: The Surface as Network Medium", *IEEE Communications Magazine*, April 2003, pp. 90-95.

[3] K.F. Laerhoven, "The Pervasive Sensor", *Proceedings of Second International Conference on Ubiquitous Computing Systems, UCS2004*, November 2004, pp. 1-5.

[4] J. Lifton, J.A. Paradiso, "Pushpin Computing System Overview: A Plattform for Distributed, Embedded, Ubiquitous Sensor networks", *Proceedings of Pervasive Computing*, LNCS 2414, Springer Verlag, 2002, pp139-151.

[5] J. Lifton, M. Broxton, J.A. Paradiso, "Experiences and Directions in Pushpin Computing", *Proceedings of 4th International Conference on Information Processing in Sensor Networks, IPSN2005*, April 2005, paper 57.

[6] H. Shinoda, N. Asamura, M. Hakozaki, X. Wang, "Two-Dimensional Signal Transmission Technology for Robotics", *Proceedings of the 2003 International Conference on Robotics and Automation*, pp. 3207-3212, September 2003.

[7] Y. Makino, K. Minamizawa, H. Shinoda, "Two Dimensional Communication Technology for Networked Sensing System", *Proceedings of International Workshop on Networked Sensing Systems 2005*, pp. 168-173, June 2005.

[8] H. Shinoda, Y. Makino, N. Yamahira, H. Itai, "Surface Sensor Network Using Inductive Signal Transmission Layer", *Proceedings of International Conference on Networked Sensing Systems 2007*, pp. 201-206, June 2007.

[9] Y. Makino, S. Ogawa, H. Shinoda, "EMG Sensor Integration Based on Two-Dimensional Communication", *Proceedings of International Conference on Networked Sensing Systems 2008*, pp. 168-173, June 2008.

[10] Van Laerhoven, et. al., "A Layered Approach to Wearable Textile Networks", *Proceedings of IEEE Eurowearable* Workshop, 2003.

[11] J. Akita, T. Shinmura, M. Toda, "Flexible Network System for Wearable Computing Using Conductive Fabric", *Proceedings of the 7th International Conference on Mobile Data Management, MDM2006*, pp. 101-104.

[12] E. Wade, H. Asada, "Conductive-Fabric Garment for a Cable-Free Body Area network", *IEEE Pervasive Computing Magazine*, January-March 2007, pp. 52-58.

[13] J. Akita, T. Shinmura, S. Sakurazawa, K. Yanagihara, M. Kunita, M. Toda, K. Iwata, "Wearable electromyography measurement system using cable-free network system on conductive fabric", *Artificial Intelligence in Medicine,* (2008) Vol. 42, pp. 99-108

[14] E.R. Wade, H. Harry Asada, "DC Powerline Communication Network for a Wearable Health Monitoring System", *Proceeedings of ISPLC 2005*, pp. 172-175.

[15] J.W. Ward, R.V. Churchill, *Complex variables and applications,* 7th edition, McGraw Hill, New York, 2004

[16] E.T. Whittaker and G.N. Watson, *A course of modern analysis*, 4th edition, Cambridge University Press, 1927.

[17] H.S. Carslaw and J.C. Jaeger, *Conduction of heat in solids*, second edition, Oxford Unversity Press, Osford, 1959.

[18] G.N. Watson, A *treatise on the theory of Bessel functions*, second edition, page 182, Cambridge University Press, 1966.